Adaptive Filtering and Control for Wavefront Reconstruction and Jitter Control in Adaptive Optics

Yu-Tai Liu, Neil Chen, and Steve Gibson

Abstract— This paper employs adaptive filtering and control for reconstruction and prediction of wavefronts and for control of laser beam jitter in an adaptive optics system. Adaptive compensation is needed in many adaptive optics applications because wind velocities and the strength of atmospheric turbulence can change rapidly, rendering any fixed-gain reconstruction algorithm far from optimal. Also, vibration of the optical platform commonly produces laser beam jitter. The performance of the methods proposed here is illustrated by application to recently developed simulations of high energy laser propagation through extended turbulence.

I. INTRODUCTION

Adaptive optics (AO) refers to the use of deformable mirrors driven by active control loops that feedback wavefront sensor (WFS) measurements to compensate for turbulence-induced phase distortion of optical waves propagating through the atmosphere [1], [2], [3], [4], [5]. These control loops reconstruct (i.e., estimate and predict) the phase profile, or wavefront, from the WFS data. The control loops in classical AO systems are linear and time-invariant (LTI), having fixed gains based on assumed statistics of atmospheric turbulence. Such control loops are not themselves adaptive, in the sense in which the term *adaptive* is used in the control and filtering community.

Adaptive compensation is needed in many AO applications because wind velocities and the strength of atmospheric turbulence can change rapidly, rendering any fixed-gain reconstruction algorithm far from optimal. Recently, adaptive wavefront reconstruction algorithms based on recursive least-squares (RLS) estimation of optimal reconstructor matrices have been proposed [6], [7], [8], [9], [10]. In this approach, an adaptive control loop augments a classical AO feedback loop. Results in [7], [8], [9], [10] have shown that the type of adaptive loops used here are robust with respect to modeling errors and sensor noise.

The real-time computational burden is a significant obstacle for adaptive wavefront reconstruction because the number of actuators and the number of sensors each can be on the order of 100 to 1000, while the digital control loops need to run at sample-and-hold rates of 1000 Hz and higher. It is a serious challenge to develop real-time adaptive algorithms with RLS parameter estimation for a problem

with so many input and output channels. For the adaptive control loops proposed in [7], [8], [10], a multichannel RLS lattice filter first presented in [11] has been reparameterized and embedded in an algorithm developed specifically for adaptive feedforward disturbance rejection in adaptive optics problems. This multichannel lattice filter preserves the efficiency and numerical stability of simpler lattices, while accommodating very large numbers of channels through a channel-orthogonalization process. Although the problem formulation and much of the structure of the adaptive control loops presented in [7], [8] and this paper do not require that a lattice filter be used for adaptive estimation of an optimal wavefront reconstructor, multichannel lattice filters do appear to be among the few classes of algorithms that can yield the speed and numerical stability required for real-time adaptive optics.

This paper presents two major advances over previous publications on the use of adaptive filtering and control in adaptive optics. First, jitter is added to the wavefront and adaptive control loops are used to suppress the jitter as well as to predict the higher-order wavefront error. In applications, jitter usually is produced by vibration of the optical bench or turbulence in the atmosphere through which the beam travels. Turbulence-induced jitter may be rather broadband, while vibration-induced jitter typically is composed of one or more narrow bandwidths produced by vibration modes of the structure supporting the optical system.

The second major advance of this paper compared to [8], [9], [12] is that the adaptive optics simulations presented here are much more realistic because a recently developed adaptive optics simulation with high-fidelity wavefront propagation model and detailed sensor characteristics, including nonlinearities, is used. Furthermore, the application is more challenging than those in [8], [9], [12] because the turbulence path is much longer.

II. ADAPTIVE OPTICS IN DIRECTED-ENERGY SYSTEMS

Figure 1 shows a schematic diagram for a generic adaptive optics problem in a directed energy system. Actuators are distributed in a two-dimensional array over a deformable mirror. These actuators are driven to adjust the profile of the mirror surface and cancel the phase distortions induced in a beam of light as it propagates through atmospheric turbulence. A wave front sensor (WFS) is used to measure the residual phase profile, using an array of subapertures that sense the spatial derivatives, or slopes, of the profile
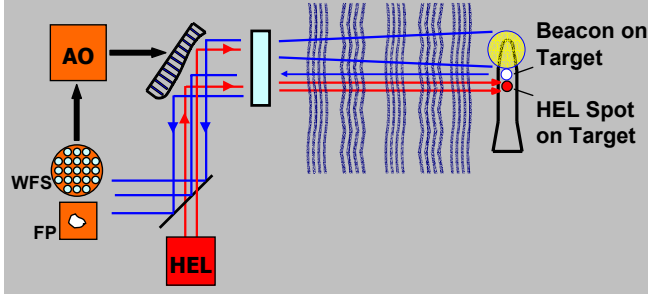
Fig. 1. Diagram of an adaptive optics problem in for a directed-energy system. Key system components: adaptive optics algorithm (AO), deformable mirror (DM), wavefront sensor (WFS), high energy laser (HEL).

on a grid interlaced with the locations of the actuators. The purpose of the AO system is to compensate the outgoing high energy laser for the wavefront error that will be induced by atmospheric turbulence, so that the laser forms a tight spot (image) on the target. The control system uses a beacon created by illuminating the target with a low energy laser as the basis for determining the commands to the deformable mirror required to cancel turbulence-induced phase distortion. Because the beacon is considered to be a distant point source, the wavefront propagating from the beacon would be very nearly a plane wave when it reached the mirror with no atmospheric turbulence. This plane wave is the desired set point for the control algorithm. If the wavefronts propagating from the beacon and to the target travel through approximately the same atmosphere, then correcting the wavefront from the beacon should compensate for the turbulence effects on outgoing beam.

For control purposes, the adaptive optics problem is represented by the block diagram in Figure 2. The measured wavefront slope vector is denoted by s. Since the wavefront cannot be measured directly, the objective of the control loops is to minimize the RMS value of the projection of s onto a certain subspace.

For the results in this paper, the jitter shown in Figure 2 is added to the track loop commands. Hence the jitter here is tilt jitter, which represents the effects on the beam control system of platform vibrations. We have experimented also with adding jitter to the deformable-mirror commands, but the results are not presented here.

The matrix V in Figure 2 represents a parameterization of actuator space [12], [13]. The actuator command vector c and the control command vector v are related by

$$c = Vv .\tag{1}$$

The matrix $\tilde{\Gamma}$ is given by

$$\tilde{\Gamma} = \Gamma V ,\tag{2}$$

where Γ is the poke matrix. Thus,

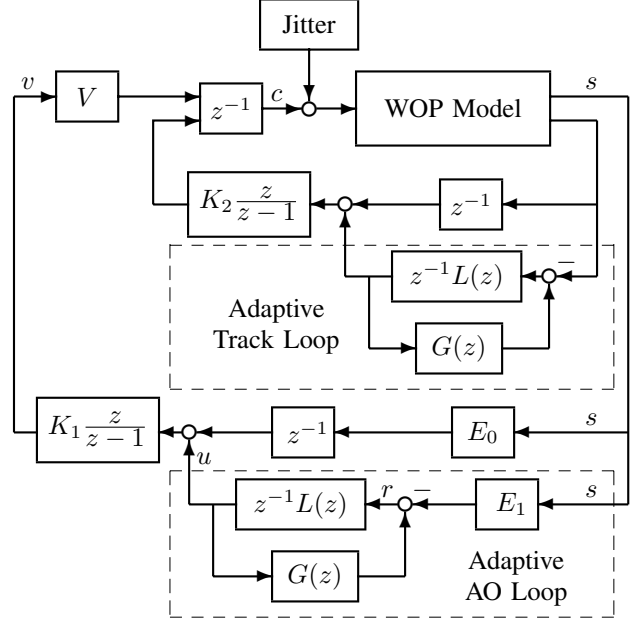$$\tilde{\Gamma} v = \Gamma c .\tag{3}$$

Fig. 2. Block diagram for adaptive optics with adaptive jitter control (top adaptive loop) and adaptive wavefront reconstruction (bottom adaptive loop).

The reconstructor matrix E_0 is a tilt-removed least-squares wavefront reconstructor, and it is assumed that

$$E_0\tilde{\Gamma} = I .\tag{4}$$

The methods described here allow the matrix E_1 to be different from E_0, but for the results here, $E_1 = E_0$.

Each z^{-1} block in Figure 2 represents a one-step delay due to sensor read-out and/or computation. Hence, the latency in the adaptive optics problem considered in this paper is two time steps, or frames.

The objective of the adaptive optics (AO) control loops is to drive the deformable mirror minimize the variance of the part of the wavefront reconstructed by E_0; i.e., the part of the wavefront in the range space of E_0. The objective of the track loops is to drive the fast-steering mirror to minimize the variance of the tilts.

The block labeled WOP (wave optics propagation) Model in Figure 2 is a high-fidelity simulation of a directed energy problem like that represented in Figure 1. This model includes the wave optics propagation of both the beacon and high energy laser beams, as well as models of the wavefront sensor and deformable mirror, and focal plane imaging on both the adaptive optics platform and the target. This wave optics model is contained in the program WaveTrain, which is a product of MZA Associates Corporation. The model used in this research is based on non-sensitive features of HEL systems.

III. The Control Loops

In the approach to adaptive optics presented here, the classical AO and track loops used in most adaptive optics

systems to date are augmented by the adaptive loops inside the dashed boxes in Figure 2. The classical and adaptive loops are described in this section.

The classical AO and track loops both contain digital integrators, with gains K_1 and K_2, respectively. For the results in this paper,

$$K_1 = K_2 = 0.5 \,. \tag{5}$$

The columns of the matrix V in Figure 2 represent the DM modes that are controlled by the AO loops in this paper. These modes are computed by a method developed in [13], which determines a set of DM modes that are orthogonal with respect to the actuator geometry (as opposed to Zernikes, which are orthogonal on the disc) and ordered according to spatial frequency. Forty of these modes are used for the results in this paper, so that the AO loops, classical and adaptive, have 40 channels each.

The adaptive AO control loop augments the classical AO loop to enhance wavefront prediction and correction, particularly for higher-order wavefront modes. The main component of this loop is the adaptive filter $L(z)$. The gains in this filter are updated adaptively. This adaptation may be either fully adaptive (i.e., at each time step) or quasi adaptive (i.e., periodically).

For identification of the adaptive filter gains, the problem is formulated as a feedforward noise-cancellation problem with tuning signal e and reference signal r. From Figure **??**,

$$r = E_1 \, s \,. \tag{6}$$

In the adaptive loop, $E_1 = E_0$ in this paper, although the methods are extended easily without this condition. The *tuning signal* for the adaptive filter is the sequence

$$e = E_0 s \,; \tag{7}$$

i.e., the adaptive filter gains are identified to minimize the variance of e. The transfer function from the control signal u to the signal e with only the classical AO loop closed is represented by $G(z)$. Of course, only an estimate of this transfer function is available in applications.

The filter L could be either FIR or IIR. While an IIR filter theoretically would produce optimal steady-state performance for stationary disturbance statistics, an FIR filter of sufficient order can approximate the steady-state performance of an IIR filter, and the convergence of the adaptive algorithm for an FIR filter is more robust with respect to modeling errors. In most adaptive optics problems to which the current methods have been applied, FIR filter orders greater than four do not offer further performance improvement. Hence, an FIR filter is used in this paper. As the gains in the filter L are updated repeatedly, and they converge to optimal constant gains when the disturbances have constant statistics.

The least-squares objective for choosing the filter matrix $L(z)$ is to minimize $e^T(t)e(t)$. An important result of the parameterization of actuator and sensor spaces in [7], [8],

[12] is that each component of $e(t)$ is affected only by the corresponding component of the control command vector v. This means that the RLS problem reduces to a set of independent RLS problems for the gains in the individual rows of $L(z)$.

A challenging feature of the problem here is the very large number of channels. Even though the parameterization of actuator and sensor spaces causes the channels in the signals v, u, and e to remain uncoupled, all channels in the noise reference r feed into each control command. Hence, the adaptive filtering problem to determine the optimal gains for $L(z)$ is multichannel. An on-line algorithm for adaptively determining the filter gains must be numerically robust in the presence of many channels. The algorithm proposed here is a multichannel adaptive lattice filter, which is based on the algorithm presented in [11].

The new adaptive track loop, which augments the standard track loop, is a two-channel version of the adaptive loop augmenting the AO loop in the bottom of Figure 2, except that in the simulations the two-channel lattice filter for the adaptive track loop has order 8, whereas the 40-channel lattice filter for the adaptive AO loop has order 4.

IV. SIMULATION RESULTS

Simulation of a problem like that illustrated in Figure 1 were performed. The high-fidelity wavefront propagation code WaveTrain simulated the effect of atmospheric turbulence on the laser beams, was wells as the optics hardware (deformable mirror and wavefront sensor). The deformable mirror in this simulation has 196 master actuators, and the Hartmann wavefront sensor had 156 subapertures. For the simulation results presented here, the beacon for adaptive optics was a point source. In current research, the control methods used here are being applied to simulations with extended beacons.

For the results presented here, two jitter bandwidths were used: 200Hz–300Hz and 200Hz–400Hz, which are beyond the bandwidths of the standard AO and track loops. Simulations were performed for four cases:

1) Only the standard AO and track loops are closed;
2) the adaptive track loop is closed but not the adaptive AO loop;
3) the adaptive AO loop is closed but not the adaptive track loop;
4) both adaptive loops are closed.

The standard AO and track loops are closed in all four cases. In cases (2)–(4), only the classical AO and track loops were closed during the first 1000 time steps. During this period, the lattice filters computed initial estimates of the optimal gains. After the adaptive loops were closed at time step 1001, the estimates of the optimal lattice-filter gains continued to converge, and Figure 5 shows, for case (4), the corresponding improvement of the on-target Strehl ratios.

For cases (1) and (4), Figure 3 shows the average intensity distributions of the on-target energy, and Figures 6 and 7 show the jitter of the target-board image. Table I compares

the peak values (long-term Strehl ratios) for the images in Figure 3 and the corresponding images for cases (2) and (3).

Perhaps the single most important performance measure for a directed energy system is the maximum accumulated energy on any single point on the target. This is the meaning of the numbers in Table I, for which the on-target intensity distributions were averaged over the last 2000 frames of the simulations. Table I shows that, in the absence of jitter, the adaptive track loop does not improve the long-term Strehl, but that in the presence of jitter, the adaptive track loop is an important complement to the adaptive AO loop.

V. CONCLUSIONS

The adaptive control loops produce significant improvement in the point spread function of the adaptive optics system. The results here have been achieved for a significantly more challenging adaptive optics problem, and a more realistic simulation model, than those used in previous studies to illustrate the effectiveness of augmenting a classical adaptive optics loop with adaptive filtering and control because the simulation with jitter used an extended turbulence path, rather than the relatively short turbulence paths common in astronomy applications. Also, the new configuration of the adaptive loops here, which use only the tracking error and closed-loop wavefront sensor vector as input to the adaptive loop, has advantages for practical implementation.

REFERENCES

[1] J. W. Hardy, "Adaptive optics," *Scientific American*, vol. 270, no. 6, pp. 60–65, 1994.

[2] G. Rousset and J. C. Fontanella et al., "First diffraction limited astronomical images with adaptive optics," *Astron. and Astrophys.*, vol. 230, pp. L29–L32, 1990.

[3] R. Q. Fugate and B. L. Ellerbroek et al., "Two generations of laser guide star adaptive optics experiments at the starfire optical range," *J. Opt. Soc. Am. A*, vol. 11, pp. 310–324, 1994.

[4] B. L. Ellerbroek, C. Van Loan, N. P. Pitsianis, and R. J. Plemmons, "Optimizing closed-loop adaptive optics performance using multiple control bandwidths," *J. Opt. Soc. Am. A*, vol. 11, pp. 2871–2886, 1994.

[5] M. Lloyd-Hart and P. McGuire, "Spatio-temporal prediction for adaptive optics wavefront reconstructors," in *Adaptive Optics* (M. Cullum, ed.), vol. ESO Conf. Proc. 54, (European Southern Observatory, Garching), pp. 95–101, 1996.

[6] B. L. Ellerbroek and T. A. Rhoadarmer, "Real-time adaptive optimization of wave-front reconstruction algorithms for closed-loop adaptive-optical systems," in *Adaptive Optical System Technologies* (D. Bonaccini and R. Tyson, eds.), vol. 3353 of *SPIE Proc.*, pp. 1174–1183, 1998.

[7] J. S. Gibson, C.-C. Chang, and B. L. Ellerbroek, "Adaptive optics: Wavefront reconstruction by adaptive filtering and control," in *38th IEEE Conference on Decision and Control*, (Phoenix, Arizona), IEEE, December 1999.

[8] J. S. Gibson, C.-C. Chang, and B. L. Ellerbroek, "Adaptive optics: wavefront correction by use of adaptive filtering and control," *Applied Optics, Optical Technology and Biomedical Optics*, pp. 2525–2538, June 2000.

[9] C.-C. Chang and J. S. Gibson, "Parallel control loops based on spatial subband processing for adaptive optics," in *American Control Conference*, (Chicago), IEEE, June 2000.

[10] Y.-T. Liu and J. S. Gibson, "Adaptive optics with adaptive filtering and control," in *American Control Conference*, (Boston, MA), June 2004.

[11] S.-B. Jiang and J. S. Gibson, "An unwindowed multichannel lattice filter with orthogonal channels," *IEEE Transactions on Signal Processing*, vol. 43, pp. 2831–2842, December 1995.

[12] J. S. Gibson, C.-C. Chang, and Neil Chen, "Adaptive optics with a new modal decomposition of actuator and sensor spaces," in *American Control Conference*, (Arlington, VA), June 2001.

[13] Y.-T. Liu, *Adaptive Optics with Adaptive Filtering and Control*. PhD thesis, UCLA, Los Angeles, CA, 2005.
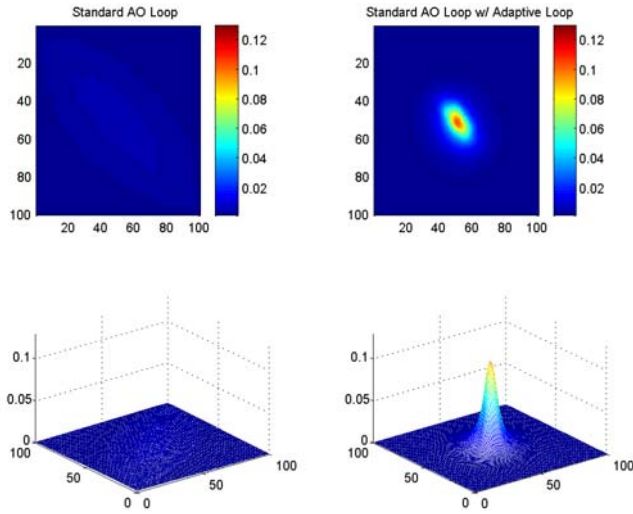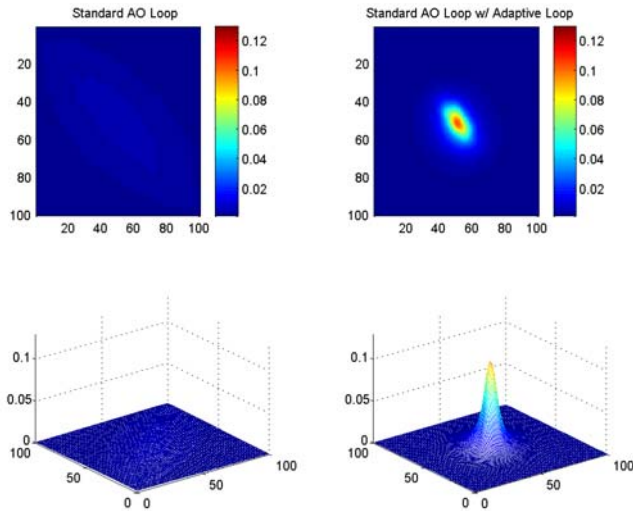
Fig. 3. Long term averaged point spread functions (top) and images (bottom) for last 2000 steps (ending at 7000), track loop jitter BW = 200 − 300 Hz. Left: starndrd AO loop, right: starndrd AO w/ adaptive track and AO loop.

Fig. 4. Long term averaged point spread functions (top) and images (bottom) for last 2000 steps (ending at 7000), track loop jitter BW = 200 − 400 Hz. Left: starndrd AO loop, right: starndrd AO w/ adaptive track and AO loop.
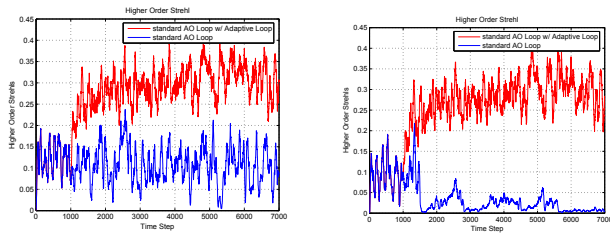

Fig. 5. Higher-order Strehl ratio time histories averaged over 50-point intervals, Adaptive loop closed at 1000. Left: track loop jitter BW = 200 − 300 Hz. right: track loop jitter BW = 200 − 400 Hz. Red: starndrd AO w/ adaptive track and AO loop; Blue: standard AO loop only.
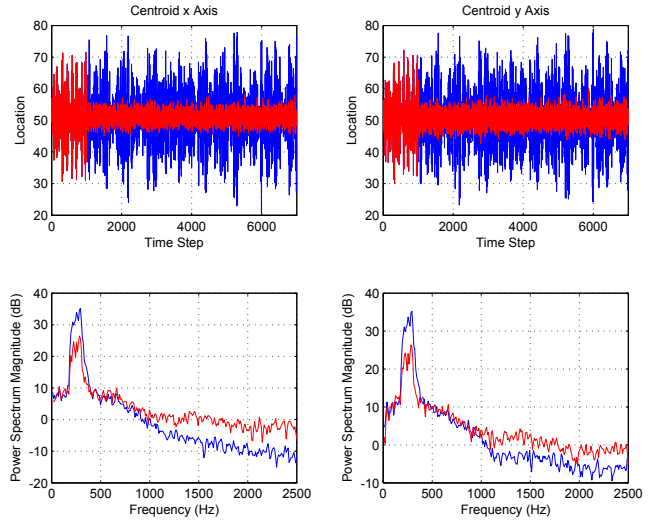

Fig. 6. Centroid of the target board image, top: time histories; bottom: power spectral density, track loop jitter BW = 200−300 Hz. Red: starndrd AO w/ adaptive track and AO loop; Blue: standard AO loop only.
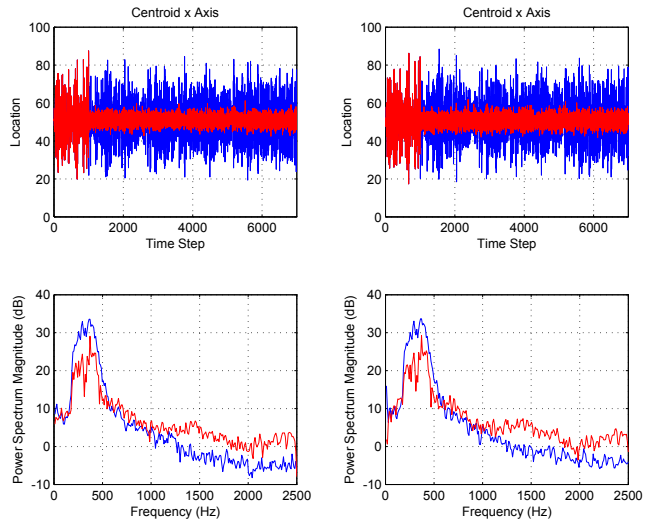

Fig. 7. Centroid of the target board image, top: time histories; bottom: power spectral density, track loop jitter BW = 200−400 Hz. Red: starndrd AO w/ adaptive track and AO loop; Blue: standard AO loop only.

Jitter Bandwidth (Hz)	No Jitter	200–300	200–400
Standard AO loop	0.1058	0.0230	0.0060
Standard AO with adaptive track loop	0.1082	0.0755	0.0661
Standard AO with adaptive AO loop	0.1836	0.0288	0.0124
Standard AO with adaptive track & AO loop	0.1825	0.1195	0.1004

TABLE I

TARGET BOARD LONG TERM STREHLS FOR 5001 : 7000 INTERVAL